



Poly(4-diphenylaminostyrene) with a well-defined polymer chain structure: Controllable optical and electrical properties

Itaru Natori*, Shizue Natori, Hiroyuki Sekikawa, Tomoyuki Takahashi, Kenji Ogino, Kousuke Tsuchiya, Hisaya Sato

Department of Organic and Polymer Materials Chemistry, Tokyo University of Agriculture & Technology, 2-24-16 Naka-cho, Koganei-city, Tokyo 184-8588, Japan

ARTICLE INFO

Article history:

Received 8 July 2009
Received in revised form
24 December 2009
Accepted 25 January 2010
Available online 2 February 2010

Keywords:

Living anionic polymerization
Poly(4-diphenylaminostyrene)
Structure and properties

ABSTRACT

The effect of polymer chain structure on the optical and electrical properties are reported for poly(4-diphenylaminostyrene) (PDAS), which was prepared by the living anionic polymerization of 4-diphenylaminostyrene (DAS) with the benzylolithium (BzLi)/*N,N,N',N'*-tetramethylethylenediamine (TMEDA) system. The optical properties of PDAS are strongly affected by the stereoregularity of the PDAS polymer chain; intramolecular excimer-forming fluorescence was observed from PDAS with a syndiotactic-rich configuration. The highest occupied molecular orbital (HOMO) and lowest unoccupied molecular orbital (LUMO) energy levels of PDAS were approximately -5.4 and -2.0 eV, respectively, regardless of the polymer chain structure. The hole and electron drift mobilities for PDAS were in the order of 10^{-4} to 10^{-5} ($\text{cm}^2/\text{V s}$) and 10^{-5} ($\text{cm}^2/\text{V s}$), respectively, with negative slopes. The distance of each triphenylamino (TPA) group in the polymer chain was a major factor influencing the drift mobility of PDAS. The current–voltage (*I*–*V*) characteristics of PDAS were controllable according to the polymer chain structure of PDAS.

© 2010 Elsevier Ltd. All rights reserved.

1. Introduction

Poly(4-diphenylaminostyrene) (PDAS), also known as poly(4-vinyltriphenylamine), has been recognized as an attractive hole-transport semiconducting polymer for opto-electronic applications, such as organic photoconductors in copy machines, electroluminescence devices, electrochromic devices, photorefractive systems, and photovoltaic devices [1–11]. It is well-known that the polymer chain structure strongly affects the properties of polymers. Therefore, a number of polymerization studies of 4-diphenylaminostyrene (DAS), a monomer of PDAS, have been carried out using anionic [1,3], radical and living radical [1,2,4–11] methods to obtain PDAS with a well-defined and controlled polymer chain structure, and to reveal the effect of polymer chain structure on the properties of PDAS.

However, the controlled polymerization of DAS is considerably difficult, even using living radical polymerization. To our knowledge, among the various effects of the polymer chain structure on the properties, only the dependence of the glass transition temperature (T_g) on the degree of polymerization of PDAS has been examined by Behl et al. [4]. Thus, only a limited amount of

information has been reported with respect to the relationship between the polymer chain structure and the properties of PDAS to date.

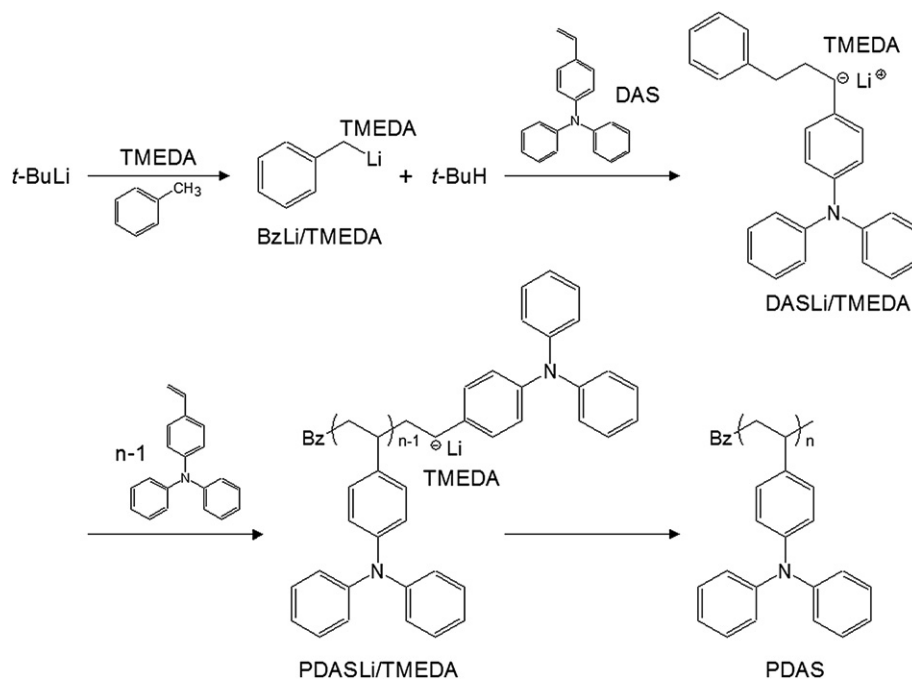
Recently, we attempted the anionic polymerization of DAS to obtain PDAS with a well-defined polymer chain structure [12,13]. As a result of our efforts, we successfully developed the first example of living anionic polymerization of DAS using the benzylolithium (BzLi)/*N,N,N',N'*-tetramethylethylenediamine (TMEDA) system, which involved the synthesis of homopolymers and block copolymers with narrow range polydispersity indices (PDI), controlled molecular weight, and well-defined polymer chain structures (Scheme 1). Furthermore, the stereoregularity of the PDAS polymer chain was revealed. In the present work, we describe the effect of polymer chain structure on the optical and electrical properties of PDAS prepared by the living anionic polymerization of DAS using the BzLi/TMEDA system.

2. Experimental section

2.1. Materials

Toluene ($\geq 99.8\%$) and TMEDA ($\geq 99.5\%$) were refluxed over calcium hydride (CaH_2 , 95%) and then distilled under dry argon. *tert*-Butyllithium (*t*-BuLi; 1.70 mol/L in pentane) and methanol (MeOH, $\geq 99.9\%$) were used without further purification. DAS was

* Corresponding author. Tel./fax: +81 42 388 7404.
E-mail address: itaru_natori@yahoo.co.jp (I. Natori).



Scheme 1. Living anionic polymerization of DAS with the BzLi/TMEDA (1.00/1.25) system in toluene.

prepared via a previously reported standard Wittig reaction [12]. All reagents were purchased from Aldrich.

2.2. General procedure for the living anionic polymerization of DAS using the BzLi/TMEDA system [12]

A well-dried 50-mL Schlenk tube was purged with dry argon, and 5.0 mL of toluene was injected at room temperature (ca. 25 °C) using a syringe. *t*-BuLi was supplied to the solution with a syringe and TMEDA was then added to the solution under dry argon, and the mixture was then stirred for 10 min to form the BzLi/TMEDA (1.00/1.25) system. DAS (0.185 mol/L solution in toluene) was added to this solution, and the reaction mixture was magnetically stirred under dry argon at room temperature. In order to terminate the reaction after polymerization, dry MeOH was injected to the reaction mixture in an equimolar amount to the lithium (Li) atoms present in the reaction mixture. The polymerization mixture was then poured into a large volume of MeOH to precipitate the polymer, which was then separated by filtration. The product was dried under reduced pressure at room temperature for 24 h, resulting in a white powdery polymer.

2.3. Measurements

The number average molecular weight (M_n), weight average molecular weight (M_w), and PDI (M_w/M_n) were determined using gel permeation chromatography (GPC) apparatus equipped with a differential refractive index (RI) detector and a Shimadzu Shim-pack GPC-80 M column (column length: 300 mm, diameter: 8 mm, effective molecular weight range: 100–4,000,000) at 40 °C. Tetrahydrofuran (THF) was used as the eluent at a flow rate of 1.0 mL/min. A molecular weight calibration curve was obtained using polystyrene (PSt) standards. ^1H nuclear magnetic resonance (NMR; Jeol ECA500) spectra of the polymers were measured in deuterated chloroform (CDCl_3) at 500 MHz. UV/vis (Shimadzu UV-3101 PC) and photoluminescence (PL; Shimadzu RF-5300 PC) spectra of the polymers were measured in dichloromethane (CH_2Cl_2 ; 10 mg/L) using quartz cells. The redox potential was

measured by cyclic voltammetry (CV) using a one-compartment cell with a polarization unit (Toho PS-06). The CV measurement was conducted for a cast film (1.0 mm) on a Pt disk working electrode (1.6 mm in diameter) in dry acetonitrile (CH_3CN) containing 0.1 M tetra-*n*-butylammonium perchlorate (Bu_4NClO_4) as an electrolyte, under dry nitrogen and at a scanning rate of 50 mV/s. A spiralled Pt wire and Ag/AgCl were used as counter and reference electrodes, respectively. The drift mobility was determined by a time-of-flight (TOF) method with a device consisting of an Al/Ti-phthalocyanine/polymer film/Au cell, a xenon flash lamp (Hamamatsu Photonics, L2359), and a digitizing oscilloscope (Gould, DSO630). The current–voltage (*I*–*V*) characteristics were measured using an electrometer (Advantest, TR-6143). The PDAS film thicknesses were determined using a profilometer (Dektak II, Solan).

3. Results and discussion

3.1. Preparation of PDAS [12]

In order to reveal the effect of polymer chain structure on the optical and electrical properties of PDAS, four types of PDAS were synthesized by the living anionic polymerization of DAS with the BzLi/TMEDA system in toluene (Scheme 1) [12]. The polymer yield for each sample was almost quantitative (>97 wt%), with PDI in a narrow range (1.10–1.22). The M_n of the polymer increased with the molar ratio of the $[\text{DAS}]_0/[\text{Li}]_0$, and the range of M_n in PDAS samples obtained was from 1680 to 54,500. The results obtained are summarized in Table 1.

The polymer chain structure of the four types of PDAS (PDAS-1 to -4) was subsequently examined using ^1H NMR spectroscopy. Fig. 1 shows typical ^1H NMR spectra for each PDAS sample obtained. The aromatic proton signals (from 6.4 to 7.4 ppm) become sharper with the increase in molecular weight. The methine proton signals around 2.3 ppm (Fig. 1a and b) are shifted to higher magnetic field (around 2.0 ppm, Fig. 1c and d), and the methylene proton signals around 1.7 ppm (Fig. 1a and b) are shifted to higher magnetic field (around 1.5 ppm, Fig. 1c and d) with increased molecular weight.

Table 1
Polymerization results of DAS with the BzLi/TMEDA (1.00/1.25) system^a.

No.	[DAS] ₀ /[Li] ₀	Yield (wt%)	<i>M</i> _n ^b	PDI ^b	I/S ^c
PDAS-1	7.50	100	1680	1.10	67/33
PDAS-2	15.0	100	3720	1.11	31/69
PDAS-3	74.0	99	21,000	1.12	6/94
PDAS-4	195	97	54,500	1.22	4/96

^a Polymerization was carried out under dry argon in toluene at room temperature for 24 h. DAS/solvent = 0.500 g/15.0 mL.

^b *M*_n and PDI were estimated by GPC, using PSt as standard.

^c The ratio of isotactic/syndiotactic structures. Determined by ¹H NMR.

The changes in the ¹H NMR spectra reflect the stereoregularity of PDAS, as well as that of PSt, as we have previously reported [12]; the methine proton signals of PDAS are shifted to higher magnetic field in the order of isotactic-, atactic-, and syndiotactic-rich polymer. The methine proton signals of isotactic PDAS and syndiotactic PDAS were around 2.3 and 2.0 ppm, respectively. The methylene proton signals of PDAS are shifted to higher magnetic field in the order of isotactic-, atactic-, and syndiotactic-rich polymer. The methylene proton signals of isotactic PDAS and syndiotactic PDAS were around 1.7 and 1.5 ppm, respectively. From the ¹H NMR spectra of Fig. 1, the methine proton signals of isotactic PDAS were ascribed to the magnetic field lower than 2.20 ppm, and the methine proton signals of syndiotactic PDAS were ascribed to that higher than 2.20 ppm. Therefore, the ratio of isotactic/syndiotactic structures (I/S) can be determined by the ratio of the area of isotactic methine proton peaks versus the area of syndiotactic methine proton peaks, and the I/S of PDAS-1 to -4 are 67/33 (isotactic-rich), 31/69 (atactic-rich), 6/94 (syndiotactic-rich), and 4/96 (syndiotactic-rich), respectively (Table 1).

3.2. Optical properties of PDAS

The UV/vis and PL spectra of PDAS-1 to -4 are shown in Fig. 2. The UV/vis spectra (Fig. 2a) show absorption bands in the region from 250 to 380 nm, and the maximum point ($\lambda_{\text{max}}^{\text{ab}}$) of each absorption was at approximately 300 nm. Therefore, the absorption

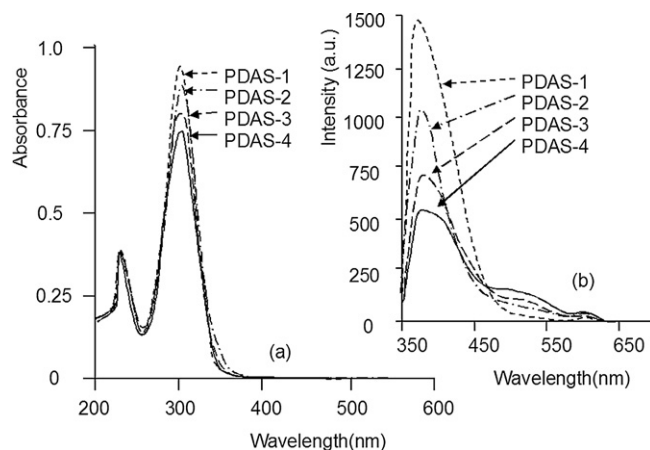


Fig. 2. UV/vis and PL spectra of PDAS: (a) UV/vis spectra of PDAS-1 to -4. [PDAS]/[CH₂Cl₂] = 0.10 mg/10.0 mL. (b) PL spectra of PDAS-1 to -4. [PDAS]/[CH₂Cl₂] = 0.10 mg/10.0 mL. Excitation wavelength of 300 nm.

in the region from 250 to 380 nm can be considered to be caused by the triphenylamino (TPA) group in the polymer chain. The intensity of the absorption becomes gradually weaker with the increase in the molecular weight and syndiotactic-rich configuration.

The emission maximum ($\lambda_{\text{max}}^{\text{em}}$) for each PL spectrum was observed in the region from 360 to 390 nm (Fig. 2b). The intensity of the $\lambda_{\text{max}}^{\text{em}}$ decreased with the increase in the molecular weight and syndiotactic-rich configuration. A broad fluorescence emission signal at approximately 520 nm was observed in the spectra of PDAS-3 and -4, due to the intramolecular excimer-forming fluorescence of PDAS [14]. The intramolecular excimer of PDAS is thought to form through the adjoining TPA groups in a syndiotactic-rich configuration, and it seems to reduce the intensity of UV/vis absorption and PL emission.

It is well-known that molecular association is a necessary condition for the formation of excimer. Therefore, TPA groups in a syndiotactic-rich configuration of PDAS (PDAS-3 and -4) are

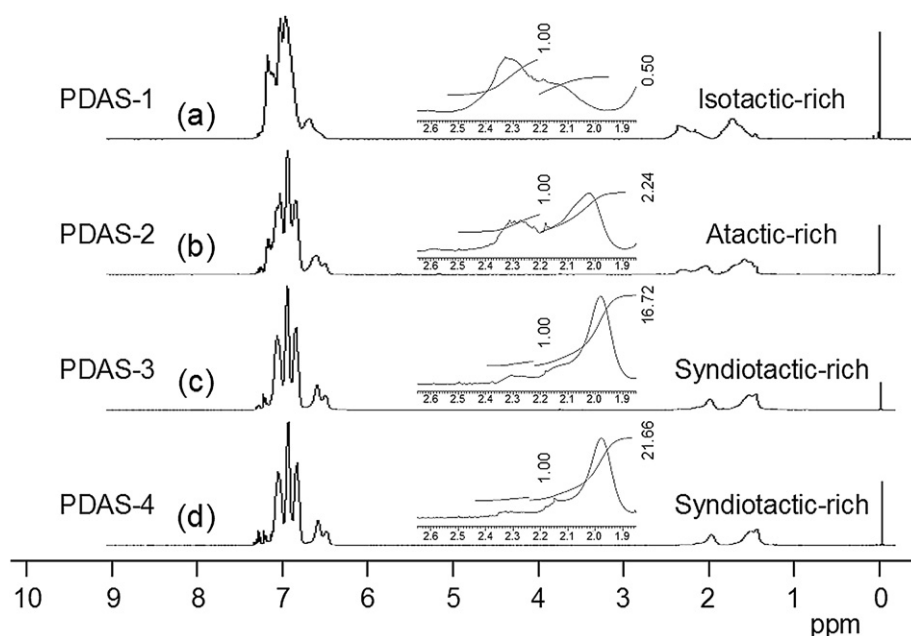


Fig. 1. ¹H NMR spectra of PDAS, obtained using the BzLi/TMEDA (1.00/1.25) system in toluene, and measured in a 3.0 wt% solution of CDCl₃ at 50 °C. (a) *M*_n = 1680, PDI = 1.10; (b) *M*_n = 3720, PDI = 1.11; (c) *M*_n = 21000, PDI = 1.12; (d) *M*_n = 54500, PDI = 1.22.

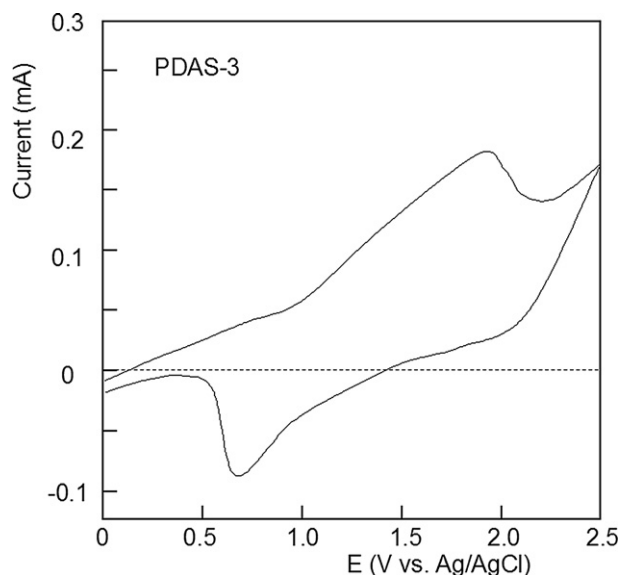


Fig. 3. Cyclic voltammogram of the PDAS-3 thin film on a Pt electrode in a solution of 0.1 M tetra-*n*-butylammonium perchlorate in dry acetonitrile (scan rate = 50 mV/s).

thought to be placed close to each other, compared with the isotactic-rich (PDAS-1) and atactic-rich (PDAS-2) configurations. That is, the distance between each TPA group in the polymer chain seems to be in the order syndiotactic-rich (PDAS-3 and -4) < atactic-rich (PDAS-2) < isotactic-rich (PDAS-1) configuration.

3.3. Electrochemical properties of PDAS

CV was performed on thin films of the PDAS-1 to -4 to reveal the effect of polymer chain structure on the electrochemical properties of PDAS. This enabled an investigation of the redox behavior of PDAS and assessment of the highest occupied molecular orbital (HOMO) and lowest unoccupied molecular orbital (LUMO) energy levels [15,16]. The peaks were referenced to Ag/AgCl and the reduction peak of ferrocene/ferrocenium (FOC).

A typical cyclic voltammogram of PDAS-3 is shown in Fig. 3. Anodic scans in the cyclic voltammograms of all samples (PDAS-1 to -4) revealed almost the same oxidation peak (E_p) around 1.9 V (vs. Ag/AgCl). The reduction peak of FOC (CH_3CN solution containing 0.1 mM FOC and 0.1 M Bu_4NClO_4) in the cathodic scan CV measurement was at 0.32 V (vs. Ag/AgCl). The HOMO energy levels of PDAS were calculated from the onset of the oxidation peak (E_{ox}), assuming that the absolute energy level of FOC is 4.8 eV below the vacuum level [15,17]. The LUMO energy level was calculated from the HOMO energy level and the absorption edge of the UV/vis

Table 2
Energy levels of PDAS.

No.	$E_{ox}(\text{V})^a$	$E_g(\text{eV})^b$	HOMO (eV vs. vacuum) ^c	LUMO (eV vs. vacuum) ^d
PDAS-1	0.91	3.44	-5.39	-1.95
PDAS-2	0.90	3.35	-5.38	-2.03
PDAS-3	0.94	3.43	-5.42	-1.99
PDAS-4	0.90	3.36	-5.38	-2.02

^a Obtained from cyclic voltammograms of PDAS (vs. Ag/AgCl).

^b Estimated from the absorption edge of UV/vis spectra.

^c The reduction peak of FOC was 0.32 V (vs. Ag/AgCl). The HOMO energy level was calculated from the onset of oxidation peak (E_{ox}) by assuming the absolute energy level of FOC is 4.8 eV below the vacuum level.

^d The LUMO energy level was calculated from the HOMO energy level and the absorption edge of UV/vis spectra.

spectra (i.e., optical band gap, E_g) for each PDAS (Fig. 2), and the results are summarized in Table 2.

The HOMO and LUMO energy levels of PDAS-1 to -4 obtained from CV and UV/vis spectra are approximately -5.4 and -2.0 eV, respectively. Therefore, it is clear that the polymer chain structure does not significantly affect the HOMO/LUMO energy levels and band gap energies of PDAS.

3.4. Influence of the polymer chain structure on drift mobility

Four kinds of the transparent polymer films with thicknesses in the order of 1.0–3.0 μm were prepared by the bar coating method using *o*-xylene solutions of PDAS-1 to -4 (polymer/*o*-xylene = 0.03 g/1.0 g). The drift mobilities, μ , of PDAS-1 to -4 films were determined using a standard TOF method, calculated according to the following equation:

$$\mu = L^2/t_T V,$$

where L is the polymer film thickness, t_T is the transit time, and V is the applied voltage. The value for t_T was determined from $\log i$ (current) vs. $\log t$ (time) plots.

The logarithm of the hole drift mobilities for PDAS-1 to -4 are plotted against the square root of the applied field [$E^{1/2}(\text{V}/\text{cm})^{1/2}$] in Fig. 4. The polymer chain structure strongly affects the hole drift mobility of PDAS. The hole drift mobility for PDAS-1 is in the order of 10^{-5} (cm^2/Vs) with a negative slope, while those for PDAS-2 to -4 are in the order of 10^{-4} to 10^{-5} (cm^2/Vs) with a negative slope. PDAS-3 and -4 exhibited almost the same hole drift mobility. An increase in the hole drift mobility was observed with an increase of the syndiotactic-rich configuration (PDAS-1 < -2 < -3 and -4), while the molecular weight did not significantly affect the hole drift mobility of PDAS (PDAS-3 and -4). In order to confirm the effect of syndiotactic structure, the hole drift mobility of PDAS samples with similar molecular weights and different tacticity (PDAS-1 and -5 [18]) were measured using standard TOF method. The results are shown in Fig. 5. The hole drift mobility was increased with an increase of the ratio of syndiotactic structure. Therefore, the syndiotactic-rich configuration in the polymer chain is a major factor that affects the hole drift mobility of PDAS.

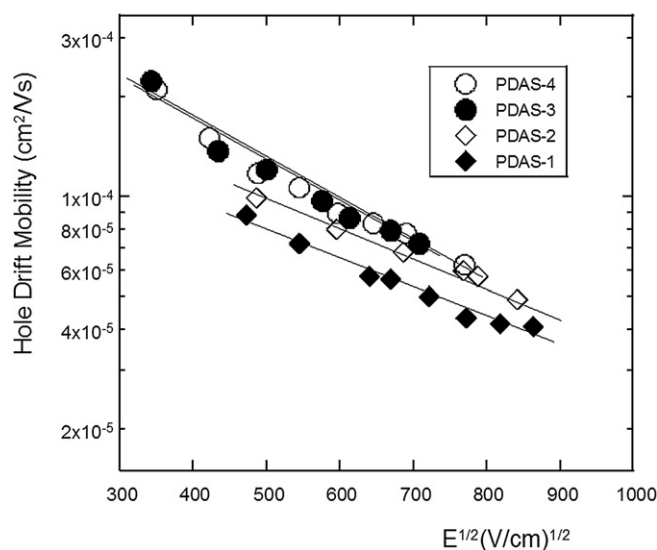


Fig. 4. Dependence of the hole drift mobility on the applied field for thin films of PDAS (PDAS-1 to -4).

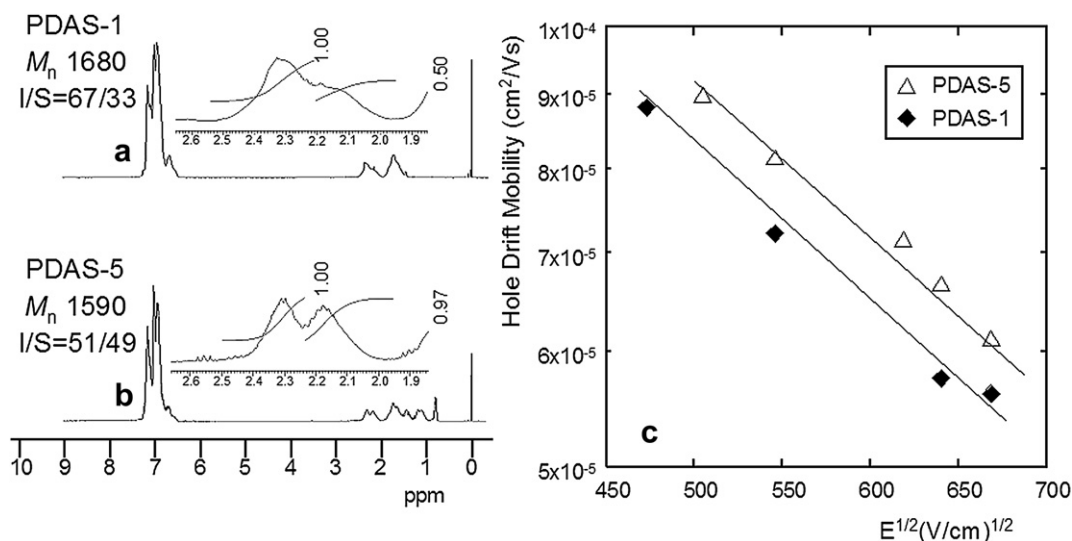


Fig. 5. ¹H NMR spectra of PDAS, obtained using the BzLi/TMEDA (1.00/1.25) system in toluene (PDAS-1) and the *n*-butyllithium (*n*-BuLi)/TMEDA (1.00/1.25) system in cyclohexane (PDAS-5), and measured in a 3.0 wt% solution of CDCl_3 at 50 °C. (a) $M_n = 1680$, PDI = 1.10; (b) $M_n = 1590$, PDI = 1.13. Dependence of the hole drift mobility on the applied field for thin films of PDAS-1 and -5 (c).

Fig. 6 shows the electron drift mobility for PDAS-1 to -4 plotted against the square root of the applied field [$E^{1/2}(\text{V/cm})^{1/2}$]. Although the electron drift mobilities for PDAS-1 to -4 are in the order of 10^{-5} (cm^2/Vs) with a negative slope, an increase in the electron drift mobility is observed with an increase of the syndiotactic-rich configuration and molecular weight (PDAS-1 < -2 < -3 < -4). Therefore, both the syndiotactic-rich configuration and molecular weight of the polymer chain seem to be important factors that affect the electron drift mobility of PDAS.

The distance between each TPA group in the polymer chain seems to be in the order syndiotactic-rich configuration < atactic-rich configuration < isotactic-rich configuration. Therefore, the drift mobility seems to be increased with the decrease of the distance between each TPA group in the polymer chain.

3.5. *I*-*V* characteristics of PDAS

The films of PDAS-1 and -3 (ca. 150 nm thick) were prepared by spin-coating *o*-xylene solutions of PDAS (polymer/*o*-

xylene = 0.03 g/1.0 g) onto indium tin oxide (ITO) glass (sheet resistance, 30 Ω), and drying under reduced pressure at room temperature for 24 h. Al (100 nm thick) was then evaporated onto the polymer layer as a cathode. The influence of polymer chain structure on the *I*-*V* characteristics of PDAS was then examined. Typical *I*-*V* characteristics for each polymer film (PDAS-1 and -3) are given in Fig. 7.

The current in PDAS-1 and -3 increased with forward bias voltage applied, showing the rectification properties. This is typical Schottky diode behavior attributed to the ohmic contact formed with ITO, while Al forms a blocking contact. The current density of PDAS-3 was significantly enhanced compared with that of PDAS-1. Thus, the syndiotactic-rich configuration of PDAS seems to considerably reduce the Schottky barrier. Therefore, the *I*-*V* characteristics of PDAS are thought to be controllable according to the polymer chain structure of PDAS.

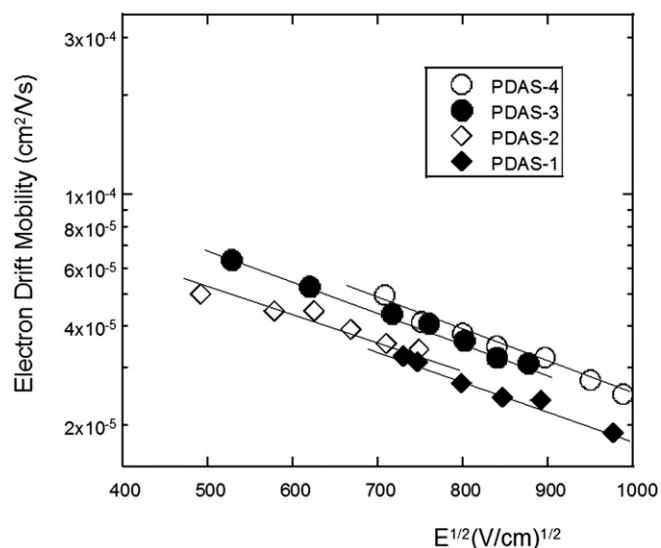


Fig. 6. Dependence of the electron drift mobility on the applied field for thin films of PDAS (PDAS-1 to -4).

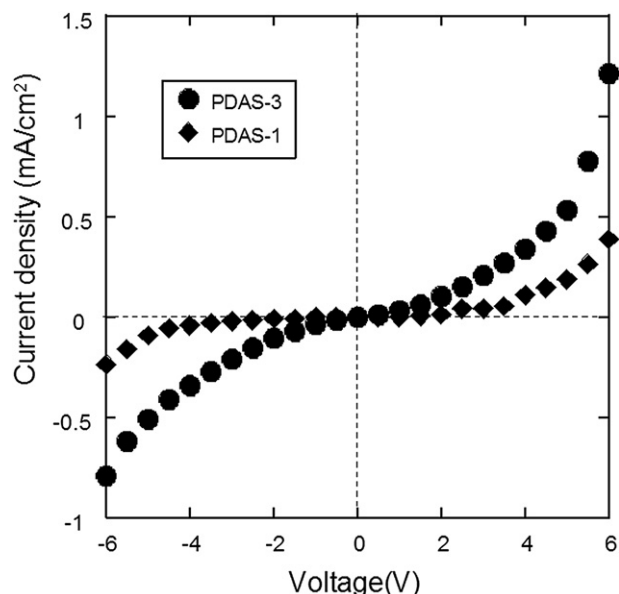


Fig. 7. *I*-*V* Characteristics of PDAS (PDAS-1 and -3) films on ITO glass.

4. Conclusion

The effect of polymer chain structure on the optical and electrical properties was examined for PDAS, which was prepared by living anionic polymerization of DAS with the *BzLi*/TMEDA system. The optical properties of PDAS were strongly affected by the stereoregularity of the PDAS polymer chain. Intramolecular excimer-forming fluorescence was observed from PDAS with a syndiotactic-rich configuration. The distance between each TPA group in the polymer chain seemed to be in the order syndiotactic-rich < atactic-rich < isotactic-rich configuration. The HOMO and LUMO energy levels of PDAS obtained from CV and UV/vis spectra were approximately -5.4 and -2.0 eV, regardless of the polymer chain structure. The polymer chain structure did not significantly affect the HOMO/LUMO energy levels and band gap energies of PDAS. The hole drift mobility of PDAS was in the order of 10^{-4} to 10^{-5} ($\text{cm}^2/\text{V s}$) with a negative slope. The electron drift mobility of PDAS was in the order of 10^{-5} ($\text{cm}^2/\text{V s}$) with a negative slope. The syndiotactic-rich configuration in the polymer chain was a major factor that influenced the drift mobility of PDAS; the drift mobility seems to be increased with the decrease of the distance between each TPA group in the polymer chain. The *I*–*V* characteristics of

PDAS were influenced by the polymer chain structure of PDAS and could be controlled accordingly.

References

- [1] Feast WJ, Peace RJ, Sage IC, Wood EL. *Polym Bull* 1999;42:167–74.
- [2] Hattemer H, Brehmer M, Zentel R, Mecher E, Müller D, Meerholz M. *Polym Prepr* 2000;41:785–6.
- [3] Tew GN, Pralle MU, Stupp SI. *Angew Chem Int Ed* 2000;39:517–21.
- [4] Behl M, Hattemer E, Brehmer M, Zentel R. *Macromol Chem Phys* 2002;203:503–10.
- [5] Lindner SM, Thelakkat M. *Macromolecules* 2004;37:8832–5.
- [6] Tsutsumi N, Murano T, Sasaki W. *Macromolecules* 2005;38:7521–5.
- [7] Lindner SM, Thelakkat M. *Macromol Chem Phys* 2006;207:2084–92.
- [8] Lindner SM, Kaufmann N, Thelakkat M. *Org Electron* 2007;8:69–75.
- [9] Lee CC, Yeh KM, Chen Y. *Polymer* 2008;49:4211–7.
- [10] Lee CC, Yeh KM, Chen Y. *J Polym Sci Part A Polym Chem* 2008;46:7960–71.
- [11] Lee CC, Yeh KM, Chen Y. *Synth Met* 2008;158:565–71.
- [12] Natori I, Natori S, Usui H, Sato H. *Macromolecules* 2008;41:3852–8.
- [13] Natori I, Natori S, Sekikawa H, Ogino K. *React Funct Polym* 2009;69:613–8.
- [14] Park MH, Huh JO, Do Y, Lee MH. *J Polym Sci Part A Polym Chem* 2008;46:5816–25.
- [15] Wu CC, Strum JC, Register RA, Tian J, Dana EP, Thompson ME. *IEEE Trans Electron Devices* 1997;44:1269–81.
- [16] Meng H, Yu W, Huang W. *Macromolecules* 1999;32:8841–7.
- [17] Bao Z, Peng Z, Galvin ME, Chandross EA. *Chem Mater* 1998;10:1201–4.
- [18] PDAS-5 was obtained by the living anionic polymerization of DAS with the *n*-BuLi/TMEDA (1.00/1.25) system in cyclohexane at room temperature for 2 h [12]. $[\text{DAS}]_0/[\text{Li}]_0 = 7.50$. DAS/solvent = 0.50 g/10.0 mL. Yield 100%, M_n 1590, PDI 1.13.